This is an open access article published under a Creative Commons Attribution (CC-BY) License, which permits unrestricted use, distribution and reproduction in any medium, provided the author and source are cited.

molecular pharmaceutics

Article

Cite This: Mol. Pharmaceutics XXXX, XXX, XXX−XXX

T_m-Values and Unfolded Fraction Can Predict Aggregation Rates for Granulocyte Colony Stimulating Factor Variant Formulations but Not under Predominantly Native Conditions

Mathew J. Robinson,[†] Paul Matejtschuk,[§] Adrian F. Bristow,[§] and Paul A. Dalby*[,†]

[†]Department of Biochemical Engineering, University College London, London WC1E 7JE, U.K.

[§]National Institute of Biological Standards and Control (NIBSC), South Mimms, Potters Bar, Hertfordshire EN6 3QG, U.K.

Supporting Information

ABSTRACT: Protein engineering and formulation optimization strategies can be taken to minimize protein aggregation in the biopharmaceutical industry. Short-term stability measures such as the midpoint transition temperature (T_m) for global unfolding provide convenient surrogates for longer-term (e.g., 2-year) degradation kinetics, with which to optimize formulations on practical time-scales. While successful in some cases, their limitations have not been fully evaluated or understood. T_m values are known to correlate with chemical degradation kinetics for wild-type granulocyte colony stimulating factor (GCSF) at pH 4−5.5. However, we found previously that the T_m of an antibody Fab fragment only correlated with its rate of monomer loss at temperatures close to the T_m. Here we evaluated T_m, the fraction of unfolded protein (f_T) at temperature T, and two additional short-term stability measures, for their ability to predict the kinetics of monomer and bioactivity loss of wild-type GCSF and four variants, at 37 °C, and in a wide range of formulations. The GCSF variants introduced one to three mutations, giving a range of conformational stabilities spanning 7.8 kcal mol^{-1}. We determined the extent to which the formulation rank order differs across the variants when evaluated by each of the four short-term stability measures. All correlations decreased as the difference in average T_m between each pair of GCSF variants increased. The rank order of formulations determined by T_m was the best preserved, with R^2-values >0.7. T_m-values also provided a good predictor (R^2 = 0.73) of the aggregation rates, extending previous findings to include GCSF variant-formulation combinations. Further analysis revealed that GCSF aggregation rates at 37 °C were dependent on the fraction unfolded at 37 °C (f_{T37}), but transitioned smoothly to a constant baseline rate of aggregation at $f_{T37} < 10^{-3}$. A similar function was observed previously for A33 Fab formulated by pH, ionic strength, and temperature, without excipients. For GCSF, all combinations of variants and formulations fit onto a single curve, suggesting that even single mutations destabilized by up to 4.8 kcal mol^{-1}, are insufficient to change significantly the baseline rate of aggregation under native conditions. The baseline rate of aggregation for GCSF under native conditions was 66-fold higher than that for A33 Fab, highlighting that they are a specific feature of each native protein structure, likely to be dependent on local surface properties and dynamics.

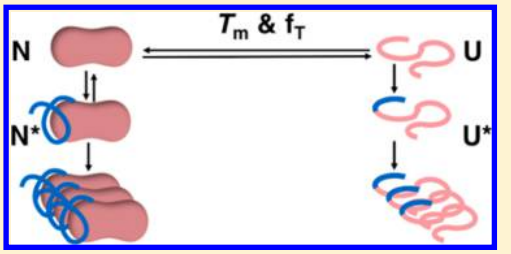

KEYWORDS: *GCSF, stability, formulation, aggregation, kinetics, protein engineering*

INTRODUCTION

Minimizing protein aggregation remains a major challenge to the biopharmaceutical industry. It can occur during protein expression,[1] downstream processing (e.g., chromatography[2] and ultrafiltration/diafiltration[3]), and during storage,[4] with aggregates treated as potentially immunogenic impurities.[5] Formulation and protein engineering each offer potential routes to enhance the shelf life of biopharmaceutical products.[6] However, it remains a major challenge to predict molecular variants and formulation excipients that improve stability, and minimize aggregation. The design process for formulation is typically semiempirical, making use of the generally observed effects of commonly used excipients, and has more recently made use of high-throughput screening in combination with design of experiments.[7] To speed development, formulation screens often depend on simple short-term stability measures to create an initial rank-ordering, prior to more resource-intensive kinetic studies at elevated temperatures, and then eventually for longer periods at lower storage temperatures. Short-term indicators of stability commonly include the onset temperature (T_{onset}), or midpoint transition temperature (T_m) for global conformational unfolding, as well as the onset temperature at which aggregates are first detected (T_{agg}).

The extent to which these short-term stability measures correlate with aggregation kinetics is not generally well characterized. T_m was found previously to correlate well with the chemical degradation kinetics for granulocyte colony stimulating factor (GCSF), across a modest range of formulation.[8] By contrast, the T_m-values for A33 Fab

Received: October 6, 2017
Revised: November 14, 2017
Accepted: November 15, 2017
Published: November 15, 2017

 © XXXX American Chemical Society

DOI: 10.1021/acs.molpharmaceut.7b00876
Mol. Pharmaceutics XXXX, XXX, XXX−XXX

formulated by pH and ionic strength correlated well with aggregation rates at elevated but not lower storage temperature.[9] Overall, the aggregation rates of A33 Fab, spanning eight orders of magnitude, were found to depend on the fraction protein unfolded until this had decreased to below approximately 10^{-4} (0.01%). At that point, the aggregation rate was broadly constant, with formulations leading to variations in the aggregation rate by just over one order of magnitude. It is not currently known whether other proteins, such as GCSF, would show similar behavior or how this would be influenced by the introduction of mutations that modify conformational stability. Understanding these features would potentially enable a convenient route for the formulation of new molecular variants, based on the best formulations identified already for the original variant. However, little is known about the relationships between protein mutations and formulation excipients in terms of the extent to which the rank order of formulations changes between closely related protein variants.

GCSF is a 19.6 kDa cytokine composed of a four-helix bundle[10] (Figure 1), and its aggregation and formulation have been studied extensively.[11−14] GCSF aggregation is thought to occur through a structurally perturbed monomer (M*), which can either revert to monomer (M), combine to form an aggregate dimer (M_2), or combine with other aggregates into larger species (M_{x+1}).[11,13,14] The aggregate dimer has not been observed directly[14] but is distinct from the reversible native dimer observed under some conditions.[13] While other proteins may undergo more complex aggregation mechanisms, partially unfolded intermediates are commonly observed on aggregation pathways.[15] Nonglycosylated GCSF is marketed as Filgrastim and is formulated in 10 mM sodium acetate, 5% sorbitol, 0.004% polysorbate-80 pH 4.0.[16] GCSF is most stable in low-pH liquid formulations, which unusually does not induce a flexible "A-state" conformation, even at pH 2.0,[12] whereas physiological pH leads to more rapid aggregation.[11,13] GCSF has been studied extensively using high-throughput methods combined with design of experiments (DoE), to generate new liquid,[17] and lyophilized[7] formulations, and also to create a range of conditions in which to assess the potential of stability measures such as T_m and T_{onset}, to predict aggregation kinetics.[8]

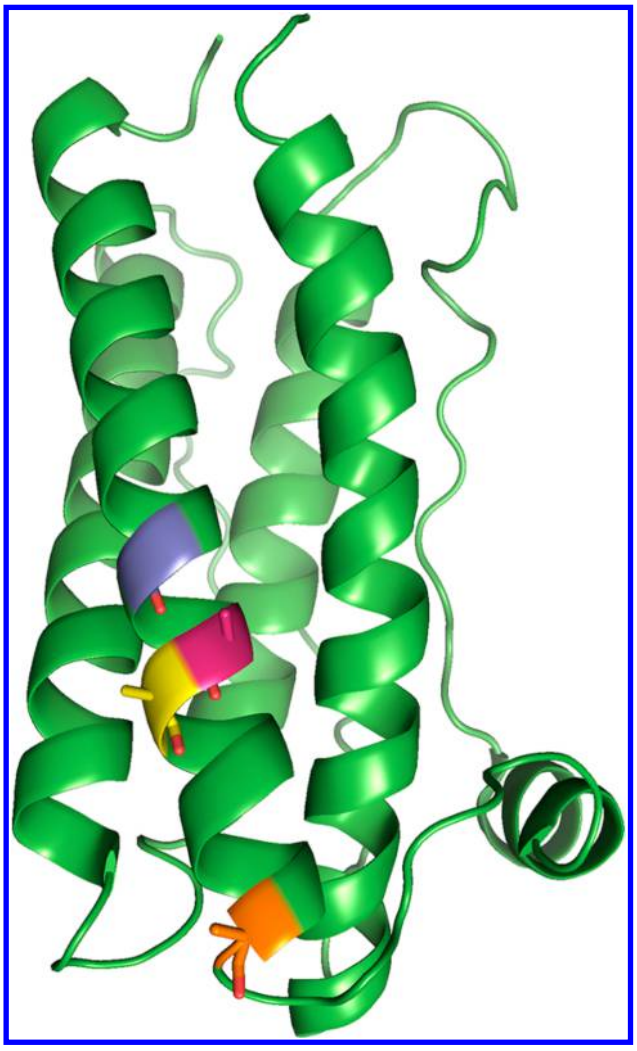

Figure 1. Location of substitutions within the structure of GCSF. Sites of alanine-to-glycine substitutions are highlighted (dark pink) A29G, (yellow) A30G, and (orange) A37G. The glycine-to-alanine substitution G26A is highlighted purple. Images generated using PyMol[18] with GCSF structure PDBID: 2D9Q.

GCSF has been engineered using several experimental and computational approaches[19] to improve or modify receptor binding[20,21] or molecular stability.[22−24] For example, the computational protein design automation (PDA) approach was used to redesigned the GCSF core and obtained mutants with thermal midpoint transitions that had increased by up to 13 °C,[22] and with no detrimental effects on receptor binding. GCSF stability has also been increased using glycine-to-alanine (G → A) mutations,[23] as these are known to increase the enthalpy of helix formation by 0.4 to 2 kcal mol^{-1}, and decrease the conformational entropy of the completely unfolded state by 0.4 kcal mol^{-1}.[25,26] G26A and G28A variants stabilized WT-GCSF with a change in the free energy of unfolding, $\Delta\Delta G_{unf}$, of −3.06 and −2.66 kcal mol^{-1}, respectively, while the G149A/G150A and G28A/G149A/G150A variants were stabilized by −4.20 and −6.16 kcal mol^{-1}, respectively.[23] Conversely, a series of alanine-to-glycine (A → G) variants of GCSF reduced the T_m from 57 °C in wild-type (WT-GCSF) to 52 °C (A30G), 47 °C (A29G/A30G), and 51 °C (A29G/A30G/A37G) and gave $\Delta\Delta G_{unf}$ values of +3.6 kcal mol^{-1} (A30G), +4.8 kcal mol^{-1} (A29G/A30G), and +4.6 kcal mol^{-1} (A29G/A30G/A37G).[24] Overall, the relatively simple tertiary structure of GCSF, the availability of several variants with altered conformational stability, and many well characterized formulations, make it an excellent system for exploring the relative impacts of protein mutations and formulation excipients on overall conformational and kinetic stability.

Previous work explored the correlation of short-term and long-term stability measures for GCSF, in a modest range of formulations that all retained a relatively stable protein (0−100 mM buffer; pH: 4.0−5.5; 0−0.05% (v/v) Tween-80; 0−5% (v/v) HP-β-CD).[8] T_m (transition midpoint) values were obtained from the statistical normalization and combination of circular dichroism, intrinsic fluorescence, ANS binding, and light scattering measurements, while degradation kinetics at 4−40 °C were also measured by an array of techniques. Under these conditions, T_m data gave very good predictions of the chemical denaturation kinetics at 4−40 °C, with an R^2 of 0.87−0.96. T_{on}, defined as the temperature at which 20% of the normalized transition was achieved, performed less well with an R^2 of 0.44−0.71 (at 4−40 °C). While very promising, a number of future improvements were highlighted such as expanding the range of formulations. Several questions also remained unanswered. For example, can other short-term measures

DOI: 10.1021/acs.molpharmaceut.7b00876
Mol. Pharmaceutics XXXX, XXX, XXX−XXX

predict the kinetics of monomer loss from aggregation? Would these also apply to the kinetics for loss of bioactivity? Given the potential of protein engineering to modify aggregation kinetics, how well do formulation rankings for one variant predict those of other related variants? Do aggregation mechanisms depend on formulation conditions (e.g., pH), and how do these changes impact on the predictive power of short-term stability measures?

Here we have used 32 formulation designs, and a series of single, double, and triple mutant variants of the nonglycosylated form of GCSF, to more broadly investigate the correlations between several short-term stability measures and degradation kinetics. The variants included WT-GCSF, as well as one stabilizing (G → A), and three destabilizing (A → G) GCSF variants (Figure 1). We examined three thermal transition measures, T_{on}, T_m, and T_{agg}, and also the fraction unfolded (f_T), determined from simultaneous measurements of static light scattering and intrinsic protein fluorescence. We compared rankings from these stability measures across the wild-type and four GCSF variants to determine how well their respective rank-ordering of 32 formulations was retained. We then also investigated the ability of the short-term measures, T_{agg}, T_m, T_{on}, and f_T, to predict the kinetics of monomer loss from GCSF aggregation and also for loss of bioactivity. This work showed that the impacts of mutations and excipients were not simply additive and revealed the extent to which rank order of formulations remain consistent across a set of protein variants that differed by only 1−3 mutations. Finally, while the work also determined which of the four short-term stability measures provided the best prediction of kinetic stability, we also found that aggregation rates measured at 37 °C were directly dependent on the fraction unfolded at 37 °C (f_{T37}) under the least stabilizing conditions, but they transitioned smoothly to a baseline rate of aggregation under conditions that retained the Native-state population at >99.9% ($f_{T37} < 10^{-3}$).

EXPERIMENTAL SECTION

Chemicals were supplied by the following manufacturers: acetic acid, HEPES, arginine monohydrochloride, glutamic acid, sucrose, and PEG 2000 (Sigma-Aldrich Co., Gillingham, UK): Tween-80, NaCl, and trehalose (Fisher Scientific Inc., Loughborough, UK), Tween-20 (Santa Cruz Biotechnology Inc., Santa Cruz, California, USA); and PEG 6000 (VWR International Ltd., Leicester, UK).

Generation of GCSF Variants. Wild-type GCSF (accession code M17706) and the A30G, A29G/A30G and A29G/A30G/A37G variants were expressed in *E. coli* BL21 DE3 from the pET21A plasmid (Novagen, WI, USA) as described previously.[24] Wild-type GCSF in the pET21A plasmid was mutated to create the G26A variant using the QuickChange Lightning Site-Directed Mutagenesis Kit (Agilent Technologies, CA, USA), with the following mutagenic primers as synthesized by Eurofins Scientific (Acton, UK): 5′-GTGAGGAAGATCCAGGCCGATGGCGCAGC-3′ (forward) and 5′-GCTGCGCCATCGGCCTGGATCTTCCTC-AC-3′ (reverse).

Mutated plasmids were transformed into XL10-Gold Ultracompetent Cells (Agilent Technologies, CA, USA) and plated onto LB agar with 0.1 mg/mL ampicillin. Colonies were picked and cultured in 5 mL of LB plus 0.1 mg/mL ampicillin at 37 °C, plasmids purified with the QIAprep Spin Miniprep Kit (Qiagen, MD, USA), then sequenced by Eurofins Scientific (Acton, UK) using standard T7 promoter and T7 terminator primers. The confirmed mutated plasmid was transformed into *E. coli* BL21 (DE3) competent cells (New England Laboratories, MA, USA) for expression.

Purification of GCSF Variants. GCSF was expressed and purified in a modified protocol to that described previously.[24] To 2 L of LB media containing 0.1 mg/mL ampicillin was added 25 mL of overnight culture of *E. coli* BL21 (DE3) (from 175 mL LB containing 0.1 mg/mL ampicillin), and then incubated at 37 °C with shaking at 150 rpm. Cells were induced at an $OD_{600\ nm}$ of 0.6 with a final concentration of 1 mM IPTG (isopropyl-thio-galacto-pyranoside), then incubated as before for a further 3.5 h before harvesting by centrifugation. Cells were resuspended in 500 mL of phosphate buffered saline (PBS), centrifuged again, and the pellet stored at −20 °C. The thawed pellet was resuspended in PBS at 10 mL per g of wet cell pellet, and sonicated (10 cycles of 15 s on and 10 s off). Lysozyme (Sigma-Aldrich Co) was then added to 1 mg/mL and the lysate allowed to roll at room temperature for 20 min. Sodium deoxycholate (Sigma-Aldrich Co) was added to 1 mg/mL and rolled for 20 min, and then benzonase (Novagen, WI, USA) added to 25 U/mL and rolled for a further 20 min. The suspension was centrifuged 18 500*g* for 30 min at 10 °C. GCSF inclusion bodies were recovered from the lysate pellet by three successive 400 mL resuspension and centrifugation steps (17 700*g* at 10 °C for 1 h, 30 min then 20 min) using (1) 50 mM Tris-HCl pH 8.0, 5 mM EDTA, 2% Triton X-100; (2) 50 mM Tris-HCl pH 8.0, 5 mM EDTA pH 8.0, 1% (w/v) sodium deoxycholate; (3) 50 mM Tris-HCl pH 8.0, 5 mM EDTA, 1 M sodium chloride. The final inclusion body pellet was resuspended in 20 mL of 2.0 M urea, the pH increased to 11.9 using dilute NaOH, then gently rolled at room temperature for 30 min. Refolding was induced by pipetting the urea solution in 1 mL steps, into 400 mL 1.0 M arginine HCl (pH 8.25), and gently rolled at room temperature overnight, then the pH adjusted to 4.25 with 50% (v/v) acetic acid. The refolded protein solution was clarified at 18 500*g* for 20 min at 10 °C. GCSF was concentrated using 3 kDa cutoff membrane centrifugal concentrators (Millipore, Watford, UK) at 3000*g* and 10 °C, to a volume of 10 mL, clarified at 18 500*g* for 15 min at 10 °C, then loaded onto a XK26/60 column (GE Healthcare, Amersham, UK) containing 350 mL of Superdex-200 media, using an Akta Explorer (GE Healthcare). GCSF was eluted after approximately 75 min (225 mL), using a mobile phase of 50 mM sodium acetate pH 4.25, at 3 mL/min, and collected as 1.8 mL fractions. GCSF was further purified by ion exchange (IEX) chromatography using a Mono-S 5/50 column (GE Healthcare) on an Akta Explorer and the mobile phase at 1 mL/min. After loading and initial washing at 100% buffer A (10 mM sodium acetate, 10 mM NaCl pH 4.25) for 5 min, GCSF was eluted using a gradient of 0−60% buffer B (10 mM sodium acetate, 1.0 M NaCl pH 4.25) over a period of 25 min, and collected as 0.5 mL fractions. GCSF variant sequences were confirmed by peptide mapping of 20 μL of 0.6 mg/mL GCSF using an Orbitrap LC-MS mass spectrometer (Thermo Fisher Scientific Inc., Loughborough, UK). Protein concentrations were determined using an extinction coefficient of 15970 M^{-1} cm^{-1} based on the protein sequence (Pace et al. 1996), and a Nanodrop-2000 (Thermo Fisher Scientific).

Design and Preparation of Formulations. For the pH studies of WT-GCSF, buffers from pH 3.5−10 were 50 mM sodium formate pH 3.5, 50 mM sodium acetate pH 4.0, 50 mM sodium acetate pH 5.0, 50 mM sodium phosphate-citrate pH 6.0, 50 mM sodium phosphate pH 7.0, 50 mM HEPES pH 8.0,

DOI: 10.1021/acs.molpharmaceut.7b00876
Mol. Pharmaceutics XXXX, XXX, XXX−XXX

Table 1. Formulation Compositions Used To Assess Stability of GCSF Variants

run	pH	ionic strength, mM	Tween-80, % (v/v)	Tween-20, % (v/v)	PEG 2000, mg/mL	PEG 6000, mg/mL	trehalose, % (w/v)	sucrose, % (w/v)	arginine, mM	glutamic acid, mM
1	4	36	0.1	0	0	0	0	3.5	0	0
2	4	86	0	0.1	0	3	0	3.5	0	50
3	4	36	0.1	0.1	0	3	0	0	50	50
4	4	86	0	0	0	0	0	0	50	0
5	8	36	0	0	0	0	0	0	0	50
6	4	86	0.1	0.1	3	0	0	0	0	50
7	8	86	0.1	0	0	0	0	3.5	50	50
8	4	36	0	0	0	3	3.5	3.5	50	50
9	4	86	0	0	3	0	3.5	3.5	0	50
10	8	86	0.1	0.1	0	3	0	0	0	0
11	8	36	0.1	0	3	3	0	3.5	0	50
12	4	36	0	0	3	3	0	0	0	0
13	8	36	0	0.1	0	3	0	3.5	50	0
14	8	36	0.1	0.1	3	0	0	0	50	0
15	4	36	0	0.1	3	0	0	3.5	50	50
16	8	86	0	0.1	0	0	3.5	0	50	50
17	4	86	0.1	0.1	0	0	3.5	3.5	50	0
18	8	86	0.1	0	3	0	3.5	0	0	0
19	8	36	0	0	3	0	3.5	3.5	50	0
20	8	86	0.1	0.1	3	3	3.5	3.5	50	50
21	4	86	0.1	0	3	3	0	3.5	50	0
22	4	36	0	0.1	0	0	3.5	0	0	0
23	4	36	0.1	0.1	3	3	3.5	3.5	0	0
24	8	36	0.1	0	0	3	3.5	0	50	0
25	8	36	0	0.1	3	3	3.5	0	0	50
26	4	36	0.1	0	3	0	3.5	0	50	50
27	8	36	0.1	0.1	0	0	3.5	3.5	0	50
28	4	86	0	0.1	3	3	3.5	0	50	0
29	8	86	0	0.1	3	0	0	3.5	0	0
30	4	86	0.1	0	0	3	3.5	0	0	50
31	8	86	0	0	3	3	0	0	50	50
32	8	86	0	0	0	3	3.5	3.5	0	0

and 50 mM CAPS pH 10.0. NaCl was added to all except the sodium phosphate buffer, to match the 110 mM ionic strength of that buffer. For the formulation studies, 28 mM of NaCl was added to 50 mM sodium acetate pH 4.0, to bring the final ionic strength to the same 36 mM as that of 50 mM HEPES pH 8.0. Design Expert 8.0 software (Stat-Ease Inc., MN, USA) was used to generate a two-level, fractional factorial, resolution IV study, with 32 runs as shown in Table 1, which assigns the conditions for each run number. Factors used were pH (4.0 or 8.0), ionic strength (36−86 mM), and excipient (0−0.1% (v/v) Tween-20, 0−0.1% (v/v) Tween-80, 0−3.0 mg/mL PEG2000, 0−3.0 mg/mL PEG6000, 0−3.5% (w/v) sucrose, 0−3.5% (w/v) trehalose, 0−50 mM arginine, and 0−50 mM glutamic acid). GCSF variants were dialyzed overnight at 4 °C against each buffer in Slide-a-Lyzer cassettes (ThermoFisher Scientific, Loughborough, UK) with a 10 kDa cutoff, centrifuged, then protein concentrations redetermined and adjusted to 0.6 mg/mL (as stocks to be used in formulations) or directly to 0.2 mg/mL (for samples with buffer only), with the appropriate buffer. Excipient stock solutions were prepared to 1.5× for each final excipient concentration, in 1× of the appropriate buffer. Each formulation was prepared from 0.67 vol excipient stock and 0.33 vol protein stock, added to 50 mL Falcon tubes for final concentrations of 0.2 mg/mL GCSF, 1× buffer, and 1× of excipients, and then filtered using 0.2 μm Corning syringe filters (Sigma-Aldrich, Gillingham, UK).

Intrinsic Protein Fluorescence and Static Light Scattering. Intrinsic protein fluorescence (IPF) (266 nm excitation, 280−450 nm emission scan) and static light scattering (SLS) at 266 and 473 nm were measured simultaneously for GCSF using an Optim-1000 (Unchained Laboratories, Wetherby, UK). measurements were taken at every 1 °C while ramping the temperature in steps from 15 to 90 °C, at 1 °C per minute. Samples were placed in three 16-well, 9 μL MCA cuvettes with rubber seals (Avacta Analytical Plc, Wetherby, UK), allowing 48 samples to be analyzed simultaneously. Each combination of variant and formulation was replicated five times. The barycentric mean fluorescence intensity, and the SLS counts, each as a function of temperature were exported into OriginPro 8.6 (Origin Lab Corp., Northampton, MA, USA), and replicates averaged prior to further analysis. Linear fits were applied to the baseline region of SLS data at the lower temperatures of the curve, and the T_{agg} (aggregation onset temperature) taken to be the first point that exceeded two standard deviations above the baseline, along with all subsequent points. The temperature dependent barycentric mean fluorescence intensities were fitted to a two-state transition using eq 1 as previously:[9]

$$I_T = I_N + aT + \frac{(I_D + bT - I_N - aT)}{1 + \exp\left(\frac{T_m - T}{m}\right)} \quad (1)$$

DOI: 10.1021/acs.molpharmaceut.7b00876
Mol. Pharmaceutics XXXX, XXX, XXX−XXX

where I_T is the observed signal, I_N and I_D are the native and denatured baseline intercepts, a and b are the native and denatured baseline slopes, T is the temperature, and T_m is the apparent midpoint of the observed thermal transition. The data fit well in all cases to this equation, and so it is assumed that protein unfolding occurs in a rapid pre-equilibrium, prior to a relatively slow aggregation step, as observed previously for GCSF,[12] and that this rate of aggregation increases with temperature to become significant on the time scale of the thermal ramping experiment when significant unfolding occurs close to T_m. T_m reflects the equilibrium conformational unfolding transition, but is convoluted partially by the aggregation rate, such that it was also dependent on the thermal ramping rate,[12] which was thus kept the same in all experiments.

The mole-fraction, f_T, of unfolded protein at any temperature T, was calculated from

$$f_T = 1 - ((I_T - I_D - bT)/(I_N + aT - I_D - bT))$$

and by substituting for I_T in eq 1, this reduces to

$$f_T = \frac{1}{1 + \exp\left(\frac{T_m - T}{m}\right)} \quad (2)$$

T_{on} was defined as the point at which 2% of protein was calculated to be unfolded, that is, where $f_{Ton} = 0.02$.

Isothermal Degradation. Wild-type GCSF and the A30G, A29G/A30G, and A29G/A30G/A37G-GCSF variants were formulated as above at 0.2 mg/mL, in 18−20 conditions selected randomly from Table 1, within 2 mL screw-cap HPLC glass vials (Chromacol Ltd., Welwyn Garden City, UK) with 0.1 mL glass microinserts (VWR International Ltd., Leicester, UK), and incubated at 37 °C. A total of 30 vials of 100 μL each, allowed for 10 sacrificial time-points with three replicates of each formulation. Mass measurements were taken before and after 37 °C degradation to confirm no evaporation of samples. Samples removed from the oven were snap-frozen and stored at −80 °C, and only allowed to be thawed once for analysis by SEC and the cell activity assay. This process was confirmed to have no measurable impact on GCSF variant monomer content or activity. Rates of monomer loss (by SEC) and activity loss (by activity) were determined as initial velocities (in % day^{-1}) by linear regression of those data between 0 and up to 20% loss in each case.

Size Exclusion Chromatography. Size exclusion chromatography (SEC) was carried out by HPLC with a 7.8 × 300 mm^2 TSKgel G3000SWXL column (Tosoh Bioscience, Redditch, UK) on an Agilent 1200 workstation (Agilent Technologies, CA, USA). Samples of 50 μL were centrifuged at 13 600*g* for 5 min, then loaded onto the column via the chilled autosampler. The mobile phase was 0.1 M phosphate pH 2.5 with a flow rate of 1 mL/min, and GCSF eluted within 25−30 min, as measured by absorbance at 214 and 280 nm. Monomer peak areas were determined by integration using the Agilent ChemStation software (Agilent Technologies) and identified by comparison to elution of an independently purified GCSF reference (NIBSC, Potters Bar, UK).

GNFS-60 Activity Assay. The GNFS-60 cell proliferation protocol for GCSF potency was carried out as described previously.[27] GNFS-60 cells were grown at 37 °C for 2−3 days, in T75 flasks (Sigma-Aldrich, Gillingham, UK), containing 20 mL of RPMI-1640 Medium (Sigma-Aldrich, Gillingham, UK), 2 ng/mL r-HuGCSF (Amgen, Uxbridge, UK), 0.5% (v/v) penicillin−streptomycin (Sigma-Aldrich, Gillingham, UK), and 5% (v/v) fetal bovine serum. Cells were spun down in 50 mL falcon tubes at 250*g* for 10 min and resuspended three times to wash out any residual GCSF, resuspending in 20 mL RPMI-1640 medium each time, and then counted with a Countess Automated Cell Counter (Invitrogen, Life Technologies Corp, Paisley, UK). A 100 μL sample of cells was added to 100 μL of 0.4% Trypan blue (Sigma-Aldrich Co, UK) at room temperature and added immediately to a cell counting chamber slide with two 10 μL chambers. The cells were diluted to a final concentration of 2 × 10^5 cells/mL.

Isothermal degradation samples were diluted in RPMI-1640 Medium to a final concentration of 4 ng/mL GCSF and 100 μL loaded into each well across one row of a sterile 96-well plate (Falcon Microtest (Corning Life Sciences B.V., Amsterdam, The Netherlands). Samples were then serially diluted into each row using RPMI-1640 Medium, and 100 μL of the 2 × 10^5 cells/mL GNFS-60 cells added to all wells, giving 15.6−2000 pg/mL final GCSF. Plates were incubated at 37 °C for 48 h, with a lid to prevent evaporation, and then 20 μL of CellTiter 96AQueous One Solution (Promega, UK) added to each well. After a further 4−5 h of incubation, the absorbance at 490 nm was measured in a platereader (Spectramax 340PC, Molecular Devices LLC, Wokingham, UK) to determine the proliferation of GNFS-60 cells.

RESULTS AND DISCUSSION

Comparison of Thermal Stability Measures T_{agg}, T_{onset}, T_m, and Fraction Unfolded, f. We used nonglycosylated wild-type (WT) GCSF to first evaluate how various short-term stability measures obtained by thermal ramping were related. These were compared across a wide range of pH to select the pH values in which to investigate further formulations. While GCSF is already known to be most stable at low pH,[11,12] we aimed deliberately to represent a wide range of stabilities and even potentially different aggregation mechanisms.

Thermal transitions were measured simultaneously by static light-scattering (SLS) at 266 nm, and by intrinsic protein fluorescence, for WT-GCSF at a range of pH from 3.5−10. SLS yielded T_{agg} values, while intrinsic fluorescence was used to obtain T_m-values, and then also the fraction unfolded, f_T, at any given temperature T. T_{on} was then defined as the temperature at which 2% protein was unfolded ($f_T = 0.02$). We then also determined the fraction unfolded at T_{agg} (f_{Tagg}) for comparison. T_m-values, measured for aggregation-prone proteins, are typically a convolution of rapid equilibrium protein unfolding, and unfolding-induced aggregation kinetics. They are thus also dependent on the thermal ramping rate, and so this was kept constant in all experiments.

As shown in Figure 2, WT-GCSF was more stable at lower pH, as determined by the higher T_m values. This is consistent with previous literature[12] in which GCSF was found not to adopt a flexible so-called "A-state" at pH 2−4, but rather exhibited increased folding and higher α-helical content (61%) at pH 4, compared to 56% at pH 7.[12] T_{on} values were always lower than T_m, by definition, and the difference between them remained constant at all pH except pH 5, indicating that the cooperativity of unfolding was generally unaffected by pH.

Surprisingly, the T_{agg} values underwent transitions at pH 3.5 and at pH 6.5 in opposite directions. T_{agg} values were below T_{on} at pH 4−6, and hence, f_{Tagg} was also low (0.5−0.8%), indicating that heat-induced aggregation of WT-GCSF began when the protein population was still predominantly native

DOI: 10.1021/acs.molpharmaceut.7b00876
Mol. Pharmaceutics XXXX, XXX, XXX−XXX

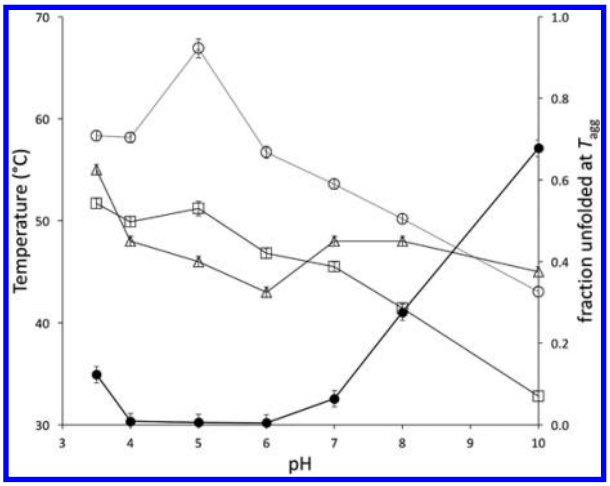

Figure 2. (Δ) T_{agg}, (○) T_m, and (□) T_{onset} temperatures for wild-type GCSF (0.2 mg/mL) at pH range 3.5−10.0. (●) Fraction unfolded at T_{agg}.

(99.2−99.5%). By contrast, T_{agg} was above T_{on} at pH 3.5 and pH 7−10, and even above T_m at pH 10. Accordingly, f_{Tagg} increased to 6−68%, indicating that heat-induced aggregation of WT-GCSF began when the population was considerably unfolded. Therefore, heat-induced aggregation for GCSF was pH-dependent, as has been observed with other proteins including A33 Fab,[9] and beta2-microglobulin.[28]

The pI of GCSF is approximately 6,[11] and so electrostatic repulsions between protein molecules would be expected to be weakest at pH 4−8. This would decrease the solubility of the protein and increase the rate of aggregation during thermal ramping, leading to the observed decrease in T_{agg}. This also meant that less unfolding could occur, before T_{agg} was reached, within the time-scale of the thermal ramping experiment. Calculations in PropKa (see Table S1, Supporting Information) actually suggest a lower magnitude for the net charge at pH 8 (−4.6), than at pH 4 (+9.9). However, such calculations ignore the impact of buffer salts on the protein net charge. The experimental data in Figure 2 suggest that the effective pI could be closer to 5, to give a true net charge at pH 8 that was slightly higher than at pH 4, and imparting greater colloidal stability to aggregation. At lower pH, our results are consistent with previous observations that GCSF aggregation is strongly influenced by an increased colloidal stability.[11]

The spike in T_m at pH 5 was linked to a T_{agg} that was the furthest below T_{on} than at any other pH, and may indicate an increased role of a native-like state in heat-induced aggregation at this pH. Unfolding from the native state was less cooperative at pH 5 than at all other pH, as indicated by the greater difference between T_{on} and T_m. SLS detected the formation of heat-induced aggregates (at T_{agg}), when only 0.5% of GCSF was unfolded. One explanation is that native GCSF has lower solubility at pH 5, in part due to being close to the pI of 6, such that a small population of native protein oligomerizes reversibly at low temperatures. For example, a reversibly formed dimer species has been reported under some conditions that does not participate in irreversible aggregation.[13] This dimer formation would effectively stabilize the native proteins against unfolding and hence increase the apparent T_m measured by intrinsic fluorescence, while not affecting T_{agg}. In general, the heat-induced aggregation of GCSF appeared to be linked to unfolding at all pH because T_{agg} was broadly within the same temperature range as T_{on} and T_m, and the lowest f_{Tagg} was 0.005 (0.5%). However, the contribution of aggregation from a native-like state could not be ruled out, particularly at pH 4−6 where f_{Tagg} was lowest. We therefore aimed to probe this further by formulating with excipients, and also combining these with protein mutations that altered the conformational stability of GCSF.

In addition to this question, T_{agg} is not necessarily expected to correlate with aggregation kinetics at lower storage temperatures, as T_{agg} is a measure of heat-induced aggregation. Therefore, we investigated the interrelationships of the various T-values, fraction unfolded (f_T), and aggregation/inactivation kinetics, across the range of formulations and mutations. We decided to limit formulations to only pH 4 and pH 8 as these had similar T_{agg} values for WT-GCSF, and yet sampled the impact of excipients upon aggregation in conditions with low ($T_{agg} < T_{on}$), and high ($T_{agg} > T_{on}$) populations of unfolded protein, respectively.

Comparison of Formulation-Averaged <T_{agg}>, <T_{onset}>, <T_m>, and <f_{Tagg}> for GCSF Variants. We purified four variants of GCSF, as described previously.[24] One single mutant (G26A) had increased conformational stability, and a series of three variants, A30G, A29G/A30G, and A29G/A30G/A37G, progressively introduced single destabilizing mutations. The destabilization of each single mutation is known to be nonadditive, such that the triple mutant variant is marginally more conformationally stable than the double mutant A29G/A30G. The synergistic effects between the A29G, A30G, and A37G mutations most likely arise from a local structural reorganization facilitated by increased flexibility and decreased α-helical propensity in the A-helix.[23] This series of variants therefore presents an opportunity to explore not only the relationship between conformational stability (ΔG) and aggregation, but also whether synergistic effects upon conformational stability translate into synergistic effects in T_{agg} or aggregation kinetics.

To discern the relationships between formulation and protein mutation effects, which are both expected to modify the conformational stability of GCSF variants, T_{agg}, T_m, T_{on}, and f_{Tagg} values were measured for all four GCSF variants plus WT-GCSF, within 32 formulations, constructed by design of experiments (DoE) as described in Table 1. Factors included pH (50 mM sodium acetate, pH 4, and 50 mM HEPES, pH 8), ionic strength (36−86 mM), polysorbate concentration (0−0.1% (v/v) Tween-20 and Tween-80), polyethylene glycol concentration (0−3 g/L PEG 2000 and PEG 6000), disaccharide concentration (0−3.5% (w/v) trehalose or sucrose), and amino-acid concentration (0−50 mM arginine or glutamic acid).

T_{agg}, T_m, T_{on}, and f_{Tagg} values in the 16 formulations at each pH, were averaged to give <T_{agg}>, <T_m>, <T_{on}>, and <f_{Tagg}> values for each variant at pH 4 and pH 8 separately, for an overall comparison in Figure 3, to the variant $\Delta\Delta G_{unf}$ (= $\Delta G_{VAR} - \Delta G_{WT}$), obtained previously at pH 4.25. These average values do not have any specific thermodynamic meaning, but allow a simple overall comparison of the behavior of the GCSF variants. For clarity, the error bars shown are standard errors of the mean for the values obtained in the 16 formulations and thus represent the precision of this mean value, whereas the actual spread that contained 95% of all the values for individual formulations, was four-times larger in all cases. At both pH 4 and pH 8, <T_m> and <T_{on}> decreased linearly as $\Delta\Delta G_{unf}$ increased. Indeed, a comparison of all

DOI: 10.1021/acs.molpharmaceut.7b00876
Mol. Pharmaceutics XXXX, XXX, XXX−XXX

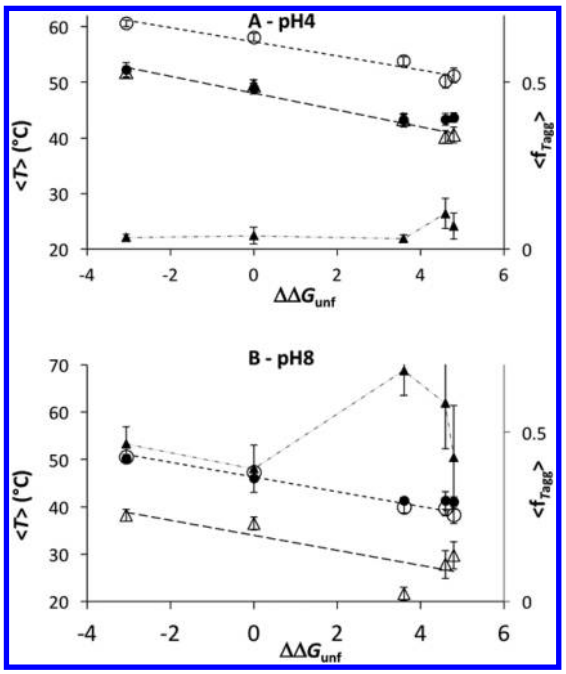

Figure 3. $\Delta\Delta G_{unf}$ of GCSF variants (WT, G26A, A30G, A29G/A30G, and A29G/A30G/A37G) as measured at pH 4.25,[24] compared to their (●) $\langle T_{agg}\rangle$, (○) $\langle T_m\rangle$, (Δ) $\langle T_{on}\rangle$ temperatures, and (▲) $\langle f_{Tagg}\rangle$, averaged across the 16 DoE formulations at (A) pH 4 and (B) pH 8. Error bars denote standard errors of the mean across the 16 formulations, each measured in triplicate. Lines of best fit are shown for (– –) $\langle T_{on}\rangle$ and (- -) $\langle T_m\rangle$, and linear interpolations are shown for (···) $\langle f_{Tagg}\rangle$.

$\Delta\Delta G_{unf}$ and $\Delta\langle T_m\rangle$ values (= $\langle T_m\rangle_{Variant2} - \langle T_m\rangle_{Variant1}$ averaged across all 32 formulations), and between all pairs of variants (including WT), gave a linear correlation with a Pearson's R^2-value of 0.98 (Figure S1, Supporting Information). This confirmed that on average, T_m reports on the conformational stability of the protein.

At pH 4, $\langle T_{agg}\rangle$ was similar to $\langle T_{on}\rangle$ for all variants including WT-GCSF, and $\langle f_{Tagg}\rangle$ remained low, indicating heat-induced aggregation from a predominantly, though not fully, native population. Only three samples had individual values of f_{Tagg} greater than 20% at pH 4, and these were for the three least stable variants, in the same formulation comprising 50 mM NaCl, 0.1% (v/v) Tween-80, 0.1% (v/v) Tween-20, 50 mM arginine, 3.5% (v/v) sucrose, and 3.5% (v/v) trehalose. The variant-averaged fraction unfolded, $\langle f_{Tagg}\rangle$, was similar for the three most stable variants of G26A (3.5%), WT (4%), and A30G (3%), but then increased to 11% and 7% in A29G/A30G/A37G and A29G/A30G, respectively, which have similar $\Delta\Delta G_{unf}$ values of 4.6 kcal mol^{-1} and 4.8 kcal mol^{-1}, respectively. This was linked to a small deviation of $\langle T_{agg}\rangle$ above $\langle T_{on}\rangle$ by 3 °C for these two variants. Essentially, $\langle T_{agg}\rangle$ remained the same from A30G to A29G/A30G/A37G and A29G/A30G, while the $\langle T_m\rangle$ and $\langle T_{on}\rangle$ values decreased. Therefore, the double and triple mutant variants retained a higher than expected $\langle T_{agg}\rangle$, indicating a retained level of stability to heat-induced aggregation, despite their lower conformational stability. The nonadditive behavior of these mutations upon $\langle T_{agg}\rangle$ may be linked to the known nonadditivity of their $\Delta\Delta G_{unf}$. However, these effects at pH 4 were relatively small overall.

At pH 8, as observed above for WT, $\langle T_{agg}\rangle \approx \langle T_m\rangle$, and $\langle f_{Tagg}\rangle$ ranged from 40 to 68%, indicating heat-induced aggregation from a significantly unfolded population in all variants. The lowest individual value of f_{Tagg} in all formulations and variants at pH 8 was 2.5%, and the highest was 99%. Interestingly, $\langle T_{agg}\rangle$ was only 2 °C lower at pH 8 than at pH 4 in all variants. However, $\langle T_m\rangle$ and $\langle T_{on}\rangle$ were lower at pH 8 than at pH 4, by 10–12 and 13 °C, respectively. Thus, while the conformational stability of GCSF variants were significantly lower at pH 8 than at pH 4, the $\langle T_{agg}\rangle$ was counterbalanced by the same colloidal effects described above for WT-GCSF. None of the variants would be expected to alter the pI of 6, and so the net charge at pH 8 would remain slightly higher than at pH 4, imparting greater colloidal stability to aggregation. Hence, a greater degree of thermal unfolding of the protein was reached at pH 8, by the time thermal ramping led to heat-induced aggregation.

The main deviations at pH 8, from linear dependencies on $\Delta\Delta G_{unf}$, were in $\langle T_{agg}\rangle$ and $\langle T_{on}\rangle$, which consequently created significant increases in $\langle f_{Tagg}\rangle$ for the three most destabilized variants. The A30G variant had an unexpectedly lower $\langle T_{on}\rangle$, indicating a considerable decrease in the cooperativity of unfolding for this variant at pH 8. This was also observed directly as shallower slopes in the unfolding transitions for formulations of this variant, as measured by intrinsic fluorescence (not shown). This observation points to a synergistic effect in which the subsequent addition of the A29G mutation compensated for the A30G mutation, and restored the unfolding cooperativity. Importantly, these effects did not impact $\langle T_{agg}\rangle$, which also did not decrease further for the most destabilizing variants. This strongly indicates colloidal stabilization effects at pH 8, which limited the impact of conformational destabilization, when comparing T_{agg}.

Overall, the generally close link between $\langle T_{agg}\rangle$, $\langle T_m\rangle$, and $\langle T_{on}\rangle$ indicated that heat-induced aggregation occurred predominantly via an unfolded state, at both pH 4 and pH 8, and in all variants. Furthermore, these results showed that for the majority of samples, the mutations did not change this predominant aggregation mechanism at either pH. However, these data were averaged from 16 formulations each, and so there may have been individual formulation-variant combinations for which the predominant aggregation mechanism was altered. Indeed, the lowest value of f_{Tagg} of 0.001%, was found for G26A at pH 4, in the presence of Tween-80, Tween-20, PEG 6000, arginine, and glutamate, suggesting an essentially native protein at T_{agg}.

Can Thermal Parameters of Formulations for One Variant Be Used To Predict Those of Another Variant?

We aimed to determine whether the rank order of formulations determined by any of the individually measured values of T_{agg}, T_m, T_{on}, or f_{Tagg} for one variant would be retained for the other variants. Such an approach could be useful where newly engineered molecular variants have promising therapeutic potential, and where the formulation data for a previous generation molecule was available. We therefore analyzed the Pearson's R^2-values for linear correlations, and Spearman's ρ-values for rank-order correlations that compared T_{agg}, T_m, T_{on}, f_{Tagg} values for the 32 formulations of each of the five variants, against those for each other variant, in all possible pairwise combinations. Spearman's correlation coefficients (ρ) were almost identical to the Pearson's linear correlation coefficients (R^2) in all cases and so the latter were adopted.

DOI: 10.1021/acs.molpharmaceut.7b00876
Mol. Pharmaceutics XXXX, XXX, XXX–XXX

To visualize these, we plotted the R^2 for each linear correlation between values from variant 1 and variant 2, against their respective $\Delta\langle T_m\rangle$ (= $\langle T_m\rangle_{Variant2} - \langle T_m\rangle_{Variant1}$). All plots are shown in Figure S2 (Supporting Information). We found that for all measures (T_{agg}, T_m, T_{on}, f_{Tagg}), the R^2-values decreased as the difference in $\langle T_m\rangle$ between the variants increased and that the smallest decrease was observed with T_m and f_{Tagg}. For T_m, the R^2-values decreased from 1 at $\Delta\langle T_m\rangle = 0$ (for all self-correlations) to 0.7, where $\Delta\langle T_m\rangle$ was < −8.8 °C (Figure 4). For f_{Tagg}, the R^2-values were retained at above 0.87

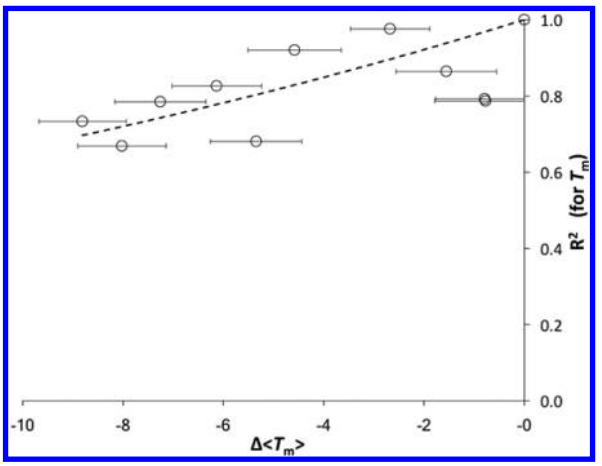

Figure 4. R^2-values obtained by linear correlation of the T_m values obtained with each formulated variant pair, decrease as their $\Delta\langle T_m\rangle$ increases. R^2-values were obtained by correlating T_m(variant 1) and T_m(variant 2), for each pair of variants obtained in all formulations. $\Delta\langle T_m\rangle = \langle T_m\rangle_{Variant2} - \langle T_m\rangle_{Variant1}$.

in 9 of 11 cases, with a value of 0.97 at $\Delta\langle T_m\rangle$ = −8.8 °C, but also two low values of 0.63 at both $\Delta\langle T_m\rangle$ = −8.0 °C and −5.3 °C. For T_{agg}, the R^2-values decreased rapidly to below 0.3 where $\Delta\langle T_m\rangle$ was < −8 °C. None of the R^2-values for T_{agg} exceeded 0.76. For T_{on}, the R^2-values were mostly in the range 0.65−0.98, but two values were low at 0.35 where $\Delta\langle T_m\rangle$ = −8 °C, and 0.5 where $\Delta\langle T_m\rangle$ = −5.3 °C, showing poor reliability. Overall, while f_{Tagg} gave the highest R^2 values on average (0.87), T_m gave the most consistent trend against $\Delta\langle T_m\rangle$, while also retaining high R^2 on average (0.8).

Our analysis demonstrated that the T_m values of any first variant of GCSF were a good prediction of those for any second variant (R^2 0.67−0.98) but that this predictive power decreased as the difference in their $\langle T_m\rangle$ increased. Such an effect indicates that as the difference in T_m (or $\Delta\Delta G_{unf}$) between two variants increases through the accumulation of mutations, then other effects such as small local structural reorganizations, also begin to modify the interaction of the protein with each of the formulation factors, in progressively less predictable ways. As discussed earlier, this effect appears to be in part due to the nonadditive impact of the combined mutations within the double and triple mutant variants, and demonstrates that even only two or three accumulated mutations can very rapidly decrease the transferability of formulation rankings between them.

The rank ordering of formulations by T_m is shown in Figure 5 for all variants, where each line links variants with the same formulation. Spearman's correlation coefficients (ρ) that compare the rank order of formulations between variants and WT-GCSF were almost identical to the Pearson's linear

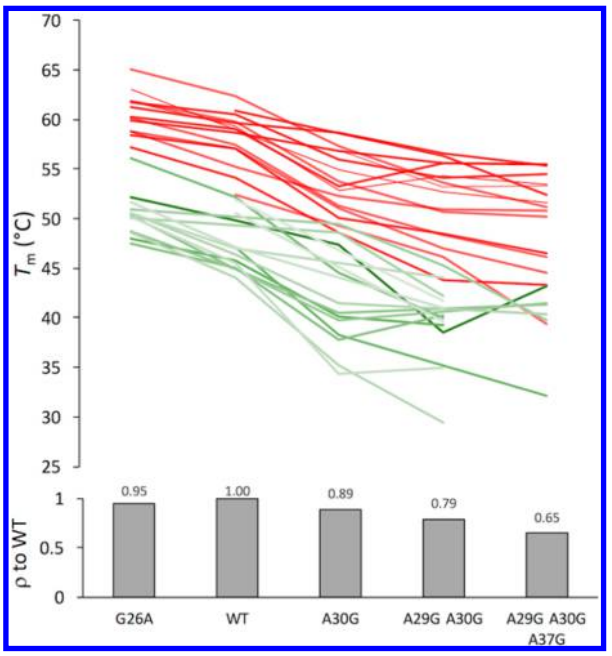

Figure 5. Comparison of formulation rank-order between variants. Top: T_m-values for each formulation. Each line links variants in the same formulation, and colored for those at pH 4 (red) and pH 8 (green). Bottom: Spearman's correlation coefficients (ρ) between the rank order of formulations for variants compared to those obtained for WT-GCSF, based on T_m values. Standard errors are omitted to retain clarity, but range from 0.1 to 1.0 °C.

correlation coefficients (R^2) in all cases. The red and green lines denote formulations at pH 4 and 8, respectively. The ρ (and R^2) values for correlations to the WT-GCSF remained above 0.65 in all cases, and as described above, generally decreased as the difference in $\langle T_m\rangle$ from that of WT-GCSF, increased.

Independent analysis of the R^2 correlations for T_m-values, in pH 4 and pH 8 formulations, each showed a similar decay with increasing $\Delta\langle T_m\rangle$ (Figure S1. Supporting Information). The R^2 values at pH 4 (0.26−0.88) were greater than those at pH 8 (0.01−0.82), but the generally lower values than those of the combined data set indicated that correlations were highly dependent upon the presence of a significant influence of pH on the T_m values, relative to the other factors investigated. Therefore, the rank-ordering of formulations created only at pH 8 would not be as readily transferrable to a second variant as those created only at pH 4.

Can T_m, T_{agg}, T_{on}, or f_{Tagg} Values for Formulations Be Used To Predict Degradation Kinetics? T_{agg}, T_m, or T_{on} values are often used as conveniently measured surrogates to rank-order formulations prior to running longer-term aggregation kinetics at lower storage temperatures. This approach was investigated previously for WT-GCSF, in a set of formulations which generally retained good protein stability,[8] and found that a T_m-value aggregated from multiple biophysical measurements gave very good predictions of chemical denaturation kinetics with an R^2 of 0.87−0.96 (at 4−40 °C). Our work expands the range of formulations and variants considerably, and so we re-evaluated the ability of T_m, but also T_{agg}, f_{Tagg}, and T_{on}, to predict aggregation kinetics.

The aggregation kinetics at 37 °C, for WT-GCSF and the variants, were monitored by SEC to track monomer loss, and also by using a cell-proliferation assay to measure the loss of

DOI: 10.1021/acs.molpharmaceut.7b00876
Mol. Pharmaceutics XXXX, XXX, XXX−XXX

bioactivity. Wild-type GCSF and the A30G, A29G/A30G, and A29G/A30G/A37G-GCSF variants were each placed into six randomly selected DoE formulations (0.2 mg/mL final concentration as used above) and incubated at 37 °C. Correlation between the initial rates of degradation from the two measures gave an R^2 of 0.65, and a slope of 0.74, indicating that the rate of activity loss was generally slower than the rate of monomer loss (Figure 6). It was possible therefore, that some

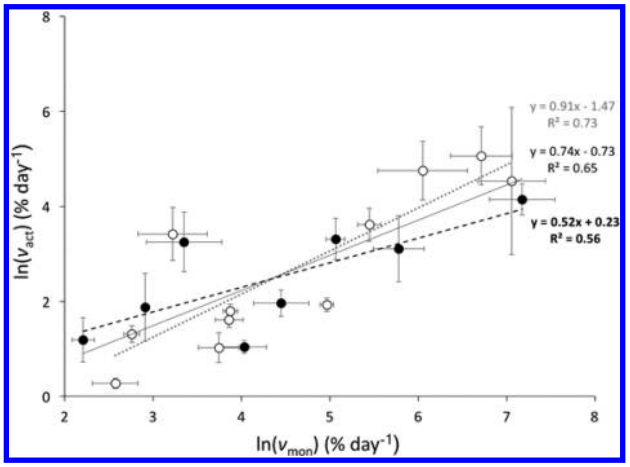

Figure 6. Comparison of initial rates of loss of activity and monomer, for GCSF WT and variants in selected formulations at 37 °C. Initial rates are plotted as natural logs for activity ($\ln(v_{act})$), and monomer loss ($\ln(v_{mon})$). Lines of best fit are shown for all formulations (○ and ●, —), and those in the absence (●,- -) and presence (○,···) of Tween 80.

of the aggregates formed, remained active, or alternatively that some of the inactive aggregates or vial surface-associated species could readily dissociate back into active soluble monomers during the bioassay. The loss of correlation could therefore have arisen if the various formulations had different impacts on the relative population or reversibility of formation of certain aggregates.

When plotting only those data for formulations that contained Tween-80, the R^2 value increased to 0.73, and the slope increased to 0.91. In the absence of Tween-80, the R^2 value was only 0.55, and the slope was only 0.5. This indicated that Tween-80 minimized any formation of reversible aggregates, or absorption to the vial surface, and hence slowed the rate of monomer loss to be more consistent with activity loss.

Linear correlations between T_{agg} or T_m, T_{on}, f_{Tagg} and the initial rates of monomer and activity loss (expressed as ln v) for each GCSF variant were determined initially using all formulations tested. T_m gave good correlations to activity and monomer loss kinetics, with R^2 values of 0.73 and 0.77, respectively. T_{on} also correlated well, with respective R^2 values of 0.67 and 0.78 to activity and monomer loss kinetics. By comparison, all T_{agg} and f_{Tagg} correlations were poor (R^2 0.17–0.52). This was mainly due to the effect of Tween-80, which modified the T_{agg} and f_{Tagg} values more significantly than the degradation rates. Figure 7 shows the separate correlations against degradation rates, for those samples with and without Tween-80, and this was generally found to improve the R^2 values. While samples with and without Tween-80 fell on distinctly separate lines for T_{agg} and f_{Tagg}, the impact of Tween-80 on plots using T_m and T_{on} was much less statistically significant. In all cases, it can be seen that Tween-80 did not significantly impact the rates of monomer loss or activity loss at 37 °C. Instead, Tween-80 increased T_{agg} by 8 °C on average, increased f_{Tagg} accordingly, and had much less impact upon T_m and T_{on}. Colloidal stabilization, as measured by T_{agg}, is expected with Tween-80, and it is often used to minimize protein–protein and protein–vial attractions and suppress the formation of aggregates.[29] It was therefore notable that colloidal stabilization by Tween-80, as measured by T_{agg}, did not influence the degradation rates at 37 °C. The stronger correlations for f_{Tagg} compared to T_{agg} for those samples with and without Tween-80 suggest that f_{Tagg} is the better indicator for colloidal stabilization, as weakened interactions between proteins would lead to a greater fraction of unfolded proteins

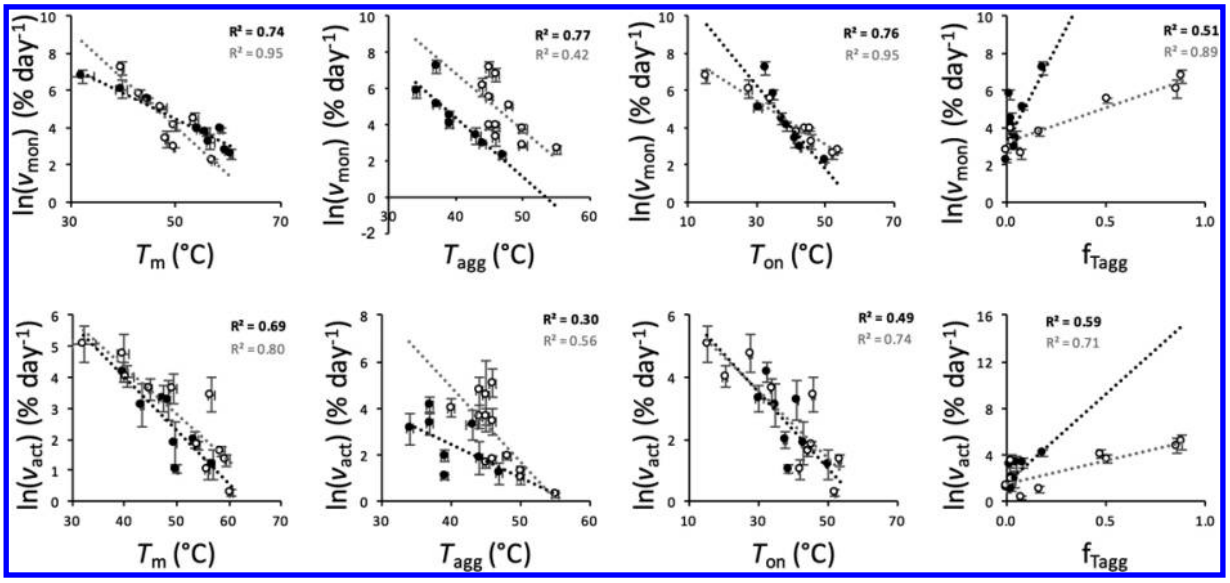

Figure 7. Evaluation of the ability of several short-term T-measures to predict the rates of monomer and activity loss for GCSF variants at 37 °C, in a random subset of the formulations. Data in the absence (●) and presence (○) of Tween-80 are fitted separately to linear functions to obtain Pearson's R^2-values shown.

DOI: 10.1021/acs.molpharmaceut.7b00876
Mol. Pharmaceutics XXXX, XXX, XXX–XXX

required to achieve the same aggregation rate at T_{agg}. Tween-80 also led to a decrease in some T_m values as expected from a mild detergent, and yet an unexpected increase in others.

These results were generally consistent with the earlier study of WT-GCSF formulations at pH 4−5.5,[8] in which T_m was found to correlate well with chemical degradation rates. Here we have shown that this extended to the comparison of formulations across single, double, and triple mutant variants with a range of conformational stabilities, and also for a pH range up to pH 8. We also found that T_{agg} and f_{Tagg} measurements were convoluted by both conformational and colloidal effects and so less able to predict degradation rates. Separation of formulations containing excipients expected to impact on colloidal stability improved the predictions, but this would not always be possible for more complex formulations.

The contrasting impact of colloidal stabilization upon the degradation kinetics at 37 °C, and upon T_{agg}, which generally occurred at higher than 37 °C, warranted further analysis. While T_{agg} measures heat-induced aggregation, and responded to the impact of Tween-80, T_m was the better predictor of GCSF formulations in terms of ranking their aggregation kinetics at 37 °C. This indicates that the aggregation kinetics of GCSF at 37 °C were strongly linked to global protein unfolding, as that is directly linked to T_m. The fraction unfolded at 37 °C (f_{T37}) was calculated from the same data as those used to determine T_m, and the influence of f_{T37} upon the initial rates of degradation are shown in Figure 8.

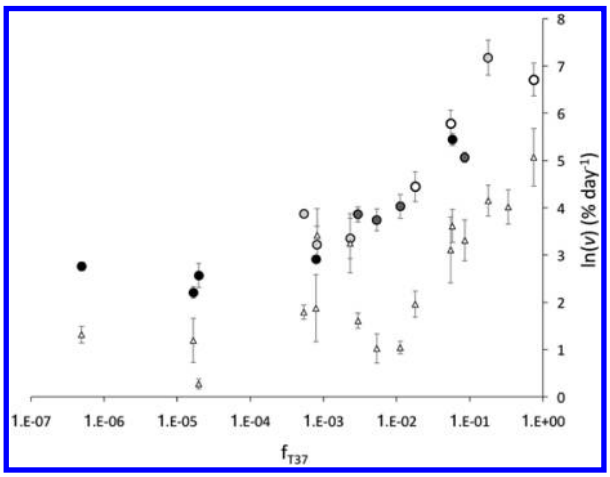

Figure 8. Dependence of initial rates of degradation upon the fraction unfolded at 37 °C for GCSF variants in a selection of formulations. Increases in the fraction unfolded at 37 °C (f_{T37}) lead to increases in the initial rates of (Δ) activity and (o) monomer loss. The rates of monomer loss are also colored by variant as (black) WT-GCSF, (dark gray) A30G, (light gray) A29G/A30G, (white) A29G/A30G/A37G. Error bars denote the standard deviation of the mean.

The initial rates of degradation, as measured by either activity or monomer loss, each generally increased with the fraction of unfolded protein at the incubation temperature of 37 °C. This was consistent with the earlier observation that heat-induced aggregation (at T_{agg}) also occurred from significantly unfolded protein populations. For a few formulations, the fraction unfolded at 37 °C fell to below 10^{-3}, and no longer influenced the degradation kinetics in this regime. The curvature in the plot indicates a mechanism switch whereby at f_{T37} above 10^{-3}, aggregation occurred predominantly via global unfolding. Then in the few conditions with f_{T37} below 10^{-3}, including most of the WT-GCSF formulations, aggregation was more likely to involve local unfolding of specific regions of the native state, as observed previously with other proteins.[9,30−32] Previous work concluded that WT-GCSF aggregation at 37 °C, pH 6.9, does not occur from the (globally) unfolded state because at 1 M sucrose (but not at 0 M), the aggregation rate was higher than the estimated diffusion limit for the globally unfolded state.[13] On the basis of a transmission coefficient of $\kappa = 1$, and a diffusion limited reaction, the reactive species was calculated to exist as one out of every million molecules in the native state ensemble.

We fitted our data for the rate of monomer loss in Figure 8 to several kinetic models and found a best fit to one that combined a diffusion-limited bimolecular reaction from a native-like state in equilibrium with the native state, with a rate-limiting monomolecular reaction from the unfolded ensemble into an aggregation-prone conformer (see Figure S3 in Supporting Information). Consistent with the previous analysis[13] discussed above, we found that under native-like conditions, the dominant aggregation mechanism was from a native-like state that was in equilibrium with the native state at one in every 200 000 native molecules (assuming a transmission coefficient of 1). Of course, not every molecular collision at the diffusion limit would necessarily lead to an aggregation event, and it is therefore likely that the transmission coefficient is much less than 1. For example, the transmission coefficient was estimated previously to be as low as 10^{-9} for irreversible aggregation between two clusters of reversibly formed antibody oligomers.[33] This would increase the population of native-like states accordingly to above one in every 200 000 and potentially by enough to become directly observable by the most sensitive biophysical techniques. For conditions or mutations that promote unfolding, the dominant aggregation mechanism became one that was rate limited by conversion of the unfolded population into an aggregation-prone conformer. The global unfolding rate itself was at least 10-fold faster than the rate of monomer loss at 37 °C and was therefore not rate limiting (see Supporting Information).

The slowest rate of monomer loss measured at 37 °C for GCSF was approximately 9% day^{-1} ($\ln \nu_{mon} = 2.2$), with $f_{T37} = 1.6 \times 10^{-5}$, and was obtained for WT in run 8. The fastest at 37 °C was approximately 1300% day^{-1} ($\ln \nu_{mon} = 7.2$), with $f_{T37} = 0.18$, and was obtained for A29G/A30G in run 19. At 4 °C, for A29G/A30G in run 19, the fraction unfolded f_{T4} would be $<1 \times 10^{-8}$, too low for diffusion-limited aggregation, and so for all variants and formulations studied, the aggregation rates at 4 °C would no longer be dependent on global protein unfolding. As the mechanism of aggregation is different at 37 and 4 °C, we would not expect the aggregation rates at 37 °C to give a good prediction of those under storage at 4 °C, as found in our previous work with A33 Fab aggregation.[9] Formulating for increased T_m values alone would thus be expected to give little improvement on the rates of aggregation under low-temperature conditions where the proteins are already more than 99.9% in the native state.

It is noteworthy that the previously reported initial rates of monomer loss under native conditions for Fab at 4−45 °C were typically less than 0.13% day^{-1} ($\ln \nu_{mon} < -2$), indicating that aggregation from the native Fab was 66-fold slower than that from native GCSF under similar conditions. These differences most likely resulted from a combination of native protein properties, such as solubility, surface hydrophobicity, net charge, local dynamics, and the accessibility of any aggregation

DOI: 10.1021/acs.molpharmaceut.7b00876
Mol. Pharmaceutics XXXX, XXX, XXX−XXX

hot-spots, rather than any differences in their global conformational stability.

Overall, as a formulation development strategy, it is useful to increase T_m in the initial stages for poorly stable proteins, at least up until the mechanistic limit is reached whereby $f_{T37} < 10^{-3}$. For degradation of GCSF at 37 °C, this limit was reached at approximately $T_m > 55$ °C, where $\ln \nu_{mon} < 4$ (% day^{-1}). Beyond that point, a very different formulation strategy would be required. Protein engineering to remove aggregation hotspots, minimize local unfolding dynamics, increase the net charge, or remove hydrophobic surface patches could be considered.

Influence of Mutational Synergies on Variant Properties. Synergistic behaviors appeared in several ways, and we infer the most likely mechanisms in the absence of further higher-order structural studies. First, loss of unfolding cooperativity in A29G at pH 8 indicated at least two conformations populated in the native state ensemble, as a result of increased backbone flexibility. Unfolding cooperativity was restored in A29G/A30G, indicating that a further increase in backbone flexibility within the same helix, fully depopulated the original native conformation found in the wild-type. Second, the $<T_m>$ for A29G/A30G formulations increased by 3.9 °C in the presence of Tween-80, whereas it decreased by 0.8 to 2.1 °C for all other variants. This points to A29G/A30G having a notably altered native state that can form stabilizing interactions with Tween-80. Finally, the conformational stability of A29G/A30G/A37G was slightly greater than for A29G/A30G, and retained the cooperative unfolding, but restored the destabilizing effects of Tween-80. The triple mutant thus appeared to have a native structure conformation similar to that in WT-GCSF.

CONCLUSION

Degradation measured by monomer loss and activity loss for GCSF at 37 °C, leading to aggregation, occurred via a population of at least 0.1% unfolded protein in most of the formulation-variant combinations studied, and the rates were closely linked to the fraction unfolded at 37 °C (f_{T37}).

T_m and the associated fraction unfolded f_T at the incubation (storage) temperature were found to be the best parameters by which to optimize formulations initially, but only up to the point at which fraction unfolded is less than approximately 0.1−1%. T_m-values provided a good predictor for activity and monomer loss kinetics (R^2 = 0.73 and 0.77, respectively) for our GCSF variant-formulation combinations (pH 4−8), extending previous findings that T_m could predict the chemical degradation rates of WT-GCSF formulations at pH 4−5. T_{agg} and f_{Tagg} measurements were less able to predict degradation rates. For example, colloidal stabilization by Tween-80 led to large increases in T_{agg} values, but it did not significantly influence the rates of monomer or activity loss for GCSF at 37 °C. Therefore, T_{agg} was useful when formulating against colloidal destabilization, but for GCSF this was only necessary in conditions where f_T was high. However, this might be expected to become more of an issue for formulations at higher protein concentrations, at lower ionic strengths, or at pH closer to the pI, and so T_{agg} would still be a useful parameter to retain in formulation screens.

The formulation rank order for one GCSF variant could be used to predict that of a second variant when based on T_m or f_{Tagg} values, but not when using T_{agg} or T_{on}. Correlations obtained between variants that differed by up to four A to G substitutions had R^2 values of 0.67−0.98, and the R^2 decreased as the difference in their $<T_m>$ increased.

The aggregation rates at 37 °C, for all variant-formulation combinations, were mechanistically dependent on the fraction unfolded at 37 °C (f_{T37}) according to a single function. Individual samples deviated from that function by up to one order of magnitude in aggregation rates due to differences in pH (4 vs 8), mutations, ionic strength, or excipients added. Such deviations were relatively minor, compared to the range of aggregation rates explored, but became very significant when fine-tuning formulations to meet clinical requirements. While the mutations progressively changed the rank order of the formulations, the rate of aggregation remained uniformly dependent upon the fraction of unfolded protein, but transitioned smoothly into a steady baseline rate of aggregation where formulations of WT-GCSF resulted in a fraction unfolded at 37 °C of less than 10^{-3}. The baseline rate of aggregation for GCSF was 66-fold higher than that determined previously with a Fab antibody fragment. These baseline rates are likely to be a specific feature of each native protein, dependent upon surface properties as well as the dynamics of local unfolding in specific regions of the native state, resulting in a native-like state that for GCSF was present potentially as low as one in every 200 000 molecules.

While the precise structural mechanisms were not confirmed, the sequential introduction of A to G mutations that would alter backbone flexibility resulted in synergistic behaviors and a fundamental impact on the formulation rank ordering. However, this nonadditive behavior did not alter the overall aggregation mechanism or the dependence of the rate of aggregation on the fraction of unfolded protein.

ASSOCIATED CONTENT

Supporting Information

The Supporting Information is available free of charge on the ACS Publications website at DOI: 10.1021/acs.molpharmaceut.7b00876.

> Comparison of $\Delta\Delta G_{unf}$ and $\Delta<T_m>$; dependence upon $\Delta<T_m>$ ($= <T_m>_{Variant2} - <T_m>_{Variant1}$) of intervariant R^2-values for each variant pair; fitting of two reaction models to dependence of initial rates of monomer loss upon fraction unfolded at 37 °C for GCSF variants in selection of formulations; calculation of net charge and pI for WT-GCSF using PropKa and structure from PDB: 2D9Q (PDF)

AUTHOR INFORMATION

Corresponding Author

*E-mail: p.dalby@ucl.ac.uk. Phone: +44 207 679 9566.

ORCID

Paul A. Dalby: 0000-0002-0980-8167

Author Contributions

The manuscript was written through contributions of all authors. All authors have given approval to the final version of the manuscript.

Notes

The authors declare no competing financial interest.

ACKNOWLEDGMENTS

The support of the Biotechnology and Biological Sciences Research Council (BBSRC) via the Bioprocess Research

DOI: 10.1021/acs.molpharmaceut.7b00876
Mol. Pharmaceutics XXXX, XXX, XXX−XXX

Industry Club (BRIC) (BB/J003824/1), and the Engineering and Physical Sciences Research Council (EPSRC) (EP/I033270/1 & EP/P006485/1) is gratefully acknowledged. We acknowledge Chris Bird (NIBSC) and Dr. Meenu Wadhwa (NIBSC) for training and support in the GCSF bioassay, and Dr. Jun Wheeler (NIBSC) for the confirmatory MS sequence analysis of the GCSF mutants.

■ ABBREVIATIONS

ANS, 8-anilinonaphthalene-1-sulfonic acid; EDTA, ethylenediaminetetraacetic acid; GCSF, granulocyte colony stimulating factor; HEPES, 4-(2-hydroxyethyl)piperazine-1-ethanesulfonic acid; HP-β-CD, hydroxypropyl-β-cyclodextrin; MCA, micro cuvette array

■ REFERENCES

(1) Espargaró, A.; Castillo, V.; de Groot, N. S.; Ventura, S. The in vivo and in vitro aggregation properties of globular proteins correlate with their conformational stability: The SH3 case. *J. Mol. Biol.* **2008**, *378*, 1116−1131.

(2) Shukla, A. A.; Gupta, P.; Han, X. Protein aggregation kinetics during Protein A chromatography: Case study for an Fc fusion protein. *J. Chrom. A* **2007**, *1171*, 22−28.

(3) Callahan, D. J.; Stanley, B.; Li, Y. Control of Protein Particle Formation During Ultrafiltration/Diafiltration Through Interfacial Protection. *J. Pharm. Sci.* **2014**, *103*, 862−869.

(4) Carpenter, J. F.; Pikal, M. J.; Chang, B. S.; Randolph, T. W. Rational Design of Stable Lyophilized Protein Formulations: Some Practical Advice. *Pharm. Res.* **1997**, *14*, 969−975.

(5) Filipe, V.; Hawe, A.; Schellekens, H.; Jiskoot, W. Aggregation and Immunogenicity of Therapeutic Proteins. In *Aggregation of Therapeutic Proteins*, 1st ed.; Wang, W., Roberts, C. J., Eds.; John Wiley & Sons, Inc.: Hoboken, NJ, 2010; pp 403−433.

(6) Voynov, V.; Chennamsetty, N.; Kayser, V.; Helk, B.; Trout, B. L. Predictive tools for stabilization of therapeutic proteins. *mAbs.* **2009**, *1*, 580−582.

(7) Grant, Y.; Matejtschuk, P.; Bird, C.; Wadhwa, M.; Dalby, P. A. Freeze drying formulation using microscale and design of experiment approaches: a case study using granulocyte colony-stimulating factor. *Biotechnol. Lett.* **2012**, *34*, 641−648.

(8) Maddux, N. R.; Iyer, V.; Cheng, W.; Youssef, A. M.; Joshi, S. B.; Volkin, D. B.; Ralston, J. P.; Winter, G.; Middaugh, C. R. High Throughput Prediction of the Long-Term Stability of Pharmaceutical Macromolecules from Short-Term Multi-Instrument Spectroscopic Data. *J. Pharm. Sci.* **2014**, *103*, 828−839.

(9) Chakroun, N.; Hilton, D.; Ahmad, S.; Platt, G.; Dalby, P. A. Mapping the Aggregation Kinetics of a Therapeutic Antibody Fragment. *Mol. Pharmaceutics* **2016**, *13*, 307−319.

(10) Hill, C. P.; Osslund, T. D.; Eisenberg, D. The structure of granulocyte-colony-stimulating factor and its relationship to other growth factors. *Proc. Natl. Acad. Sci. U. S. A.* **1993**, *90*, 5167−5171.

(11) Chi, E. Y.; Krishnan, S.; Kendrick, B. S.; Chang, B. S.; Carpenter, J. F.; Randolph, T. W. Roles of conformational stability and colloidal stability in the aggregation of recombinant human granulocyte colony-stimulating factor. *Protein Sci.* **2003**, *12*, 903−913.

(12) Kolvenbach, C. G.; Narhi, L. O.; Philo, J. S.; Li, T.; Zhang, M.; Arakawa, T. Granulocyte-colony stimulating factor maintains a thermally stable, compact, partially folded structure at pH 2. *J. Pept. Res.* **1997**, *50*, 310−318.

(13) Krishnan, S.; Chi, E. Y.; Webb, J. N.; Chang, B. S.; Shan, D.; Goldenberg, M.; Manning, M. C.; Randolph, T. W.; Carpenter, J. F. Aggregation of Granulocyte Colony Stimulating Factor under Physiological Conditions: Characterization and Thermodynamic Inhibition. *Biochemistry* **2002**, *41*, 6422−6431.

(14) Raso, S. W.; Abel, J.; Barnes, J. M.; Maloney, K. M.; Pipes, G.; Treuheit, M. J.; King, J.; Brems, D. N. Aggregation of granulocyte-colony stimulating factor in vitro involves a conformationally altered monomeric state. *Protein Sci.* **2005**, *14*, 2246−2257.

(15) Wang, W.; Nema, S.; Teagarden, D. Protein aggregation—Pathways and influencing factors. *Int. J. Pharm.* **2010**, *390*, 89−99.

(16) Herman, A.; Boone, T.; Lu, H. Characterization, Formulation, and Stability of Neupogen (Filgrastim), a Recombinant Human Granulocyte-Colony Stimulating Factor. In *Formulation, Characterization, and Stability of Protein Drugs: Case Histories*; Pearlman, R., Wang, Y. J., Eds.; Springer: Boston, MA, 2002; pp 303−328.

(17) Ablinger, E.; Hellweger, M.; Leitgeb, S.; Zimmer, A. Evaluating the effects of buffer conditions and extremolytes on thermostability of granulocyte colony-stimulating factor using high-throughput screening combined with design of experiments. *Int. J. Pharm.* **2012**, *436*, 744−752.

(18) DeLano, W. L. *The PyMOL Molecular Graphics System*; Schrodinger, 2017. http://www.pymol.org (accessed May 24, 2017).

(19) Vignesh, S. N.; Narayanan, S.; Sivanandha, M. Mutational Analysis on Human Granulocyte Macrophage-Colony Stimulating Factor Stability Using Computational Approaches. *Trends Bioinf.* **2015**, *8*, 1−13.

(20) Sarkar, C. A.; Lowenhaupt, K.; Horan, T.; Boone, T. C.; Tidor, B.; Lauffenburger, D. A. Rational cytokine design for increased lifetime and enhanced potency using pH-activated histidine switching. *Nat. Biotechnol.* **2002**, *20*, 908−913.

(21) Sarkar, C. A.; Lowenhaupt, K.; Wang, P. J.; Horan, T.; Lauffenburger, D. A. Parsing the Effects of Binding, Signaling, and Trafficking on the Mitogenic Potencies of Granulocyte Colony-Stimulating Factor Analogues. *Biotechnol. Prog.* **2003**, *19*, 955−964.

(22) Luo, P.; Hayes, R. J.; Chan, C.; Stark, D. M.; Hwang, M. Y.; Jacinto, J. M.; Juvvadi, P.; Chung, H. S.; Kundu, A.; Ary, M. L.; Dahiyat, B. I. Development of a cytokine analog with enhanced stability using computational ultrahigh throughput screening. *Protein Sci.* **2002**, *11*, 1218−1226.

(23) Bishop, B.; Koay, D. C.; Sartorelli, A. C.; Regan, L. Reengineering Granulocyte Colony-stimulating Factor for Enhanced Stability. *J. Biol. Chem.* **2001**, *276*, 33465−33470.

(24) Bristow, A. F.; Bird, C.; Bolgiano, B.; Thorpe, R. Regulatory requirements for therapeutic proteins: the relationship between the conformation and biological activity of filgrastim. *Pharmeur. Bio. Sci. Notes.* **2012**, 103−17.

(25) Chakrabartty, A.; Baldwin, R. L. Stability of α-Helices. *Adv. Protein Chem.* **1995**, *46*, 141−176.

(26) Scott, K. A.; Alonso, D. O.; Sato, S.; Fersht, A. R.; Daggett, V. Conformational entropy of alanine versus glycine in protein denatured states. *Proc. Natl. Acad. Sci. U. S. A.* **2007**, *104*, 2661−2666.

(27) Levy, M. J.; Gucinski, A. C.; Sommers, C. D.; Ghasriani, H.; Wang, B.; Keire, D. A.; Boyne, M. T. Analytical techniques and bioactivity assays to compare the structure and function of filgrastim (granulocyte-colony stimulating factor) therapeutics from different manufacturers. *Anal. Bioanal. Chem.* **2014**, *406*, 6559−6567.

(28) Gosal, W. S.; Morten, I. J.; Hewitt, E. W.; Smith, D. A.; Thomson, N. H.; Radford, S. E. Competing Pathways Determine Fibril Morphology in the Self-assembly of β2-Microglobulin into Amyloid. *J. Mol. Biol.* **2005**, *351*, 850−864.

(29) Wang, W. Instability, stabilization, and formulation of liquid protein pharmaceuticals. *Int. J. Pharm.* **1999**, *185*, 129−188.

(30) Dobson, C. M. Protein folding and misfolding. *Nature* **2003**, *426*, 884−890.

(31) Uversky, V. N.; Li, J.; Fink, A. L. Evidence for a Partially Folded Intermediate in α-Synuclein Fibril Formation. *J. Biol. Chem.* **2001**, *276*, 10737−10744.

(32) Zhuravlev, P. I.; Reddy, G.; Straub, J. E.; Thirumalai, D. Propensity to Form Amyloid Fibrils Is Encoded as Excitations in the Free Energy Landscape of Monomeric Proteins. *J. Mol. Biol.* **2014**, *426*, 2653−2666.

(33) Arosio, P.; Rima, S.; Lattuada, M.; Morbidelli, M. Population balance modeling of antibodies aggregation kinetics. *J. Phys. Chem. B* **2012**, *116*, 7066−7075.

DOI: 10.1021/acs.molpharmaceut.7b00876
Mol. Pharmaceutics XXXX, XXX, XXX−XXX